New Insight Into the Evaluation of Abnormal Left Ventricular Wall Motion

Yoichi Nakamura (y.nakamura@soyokaze-cvd.jp)
Soyokaze CardioVascular Medicine and Diabetes Care

Research

Keywords: Heart failure, Centroid, Dyssynchrony, Left ventricle, Echocardiography, Cardiac resynchronization therapy

Posted Date: February 19th, 2021

DOI: https://doi.org/10.21203/rs.3.rs-218811/v1

Abstract

Background

Evaluation of mechanical dyssynchrony using echocardiography has failed to improve refractory heart failure in patients treated with cardiac resynchronization therapy. Previous predictors may not accurately reflect cardiac dyssynchrony. It was hypothesized that the spatially and temporary continuous information of the whole endocardium is required when the mechanical dyssynchrony is assessed using echocardiography. This study aimed to examine differences in the locus of the centroid of the left ventricle between abnormal and normal wall motion.

Methods

Twenty-seven patients with dilated cardiomyopathy (left ventricular ejection fraction [LVEF]: 43±7%) and 45 old myocardial infarction patients with aneurysm (LVEF: 38±11%) were compared with 188 individuals with normal wall motions (LVEF: 61±5%). In an off-line system, the border of the endocardium was defined for each coordinate via the two-dimensional speckle tracking method. The centroid of the three-dimensional left ventricle was defined as the central point between both centroids calculated from four- and two-chamber images using an original application.

Results

The locus of the centroid of the left ventricle in the normal wall motion group showed a horizontally inverted β shape, whereas this shape was absent in the other groups. When corrected by left ventricular end-systolic volume, the total and each directional length of the locus of the centroid of the left ventricle in the abnormal wall motion groups were clearly reduced compared with those recorded in the normal wall motion group. The acceleration of the centroid was also reduced in the abnormal wall motion groups. Multiple regression analysis with a stepwise method revealed a corrected antero-posterior shift of the centroid of left ventricle by left ventricular end-systolic volume and N-terminal pro-brain natriuretic peptide, which strongly correlated with the LVEF (adjusted R^2: 0.6818, $p \leq 2.2e\text{-}16$).

Conclusion

Use of the locus of the centroid of the left ventricle provides novel insight into the evaluation of abnormal left ventricular contractions.

Trial registration

retrospectively registered

Background

In the last century, echocardiography emerged in the clinical field as a visualization tool for the evaluation of cardiac anatomical and pathological abnormalities, as well as the flow dynamics of heart diseases [1].

With the technological development, this diagnostic tool has contributed to the evaluation of cardiac diseases, such as cardiomyopathies, ischemic heart diseases, valvular heart diseases, etc. However, despite the application of several techniques, the objective judgement of the left ventricular (LV) wall motion remains a challenge.

For example, it is recognized that cardiac resynchronization therapy is a therapeutic strategy for patients with medical resistant refractory heart failure in whom LV systolic function is severely reduced. The European Society of Cardiology guidelines established in 2016 and 2019 stated that patients with a symptomatic sinus rhythm, reduced LV ejection fraction (LVEF), prolonged conduction time which met the QRS duration ≥ 130 ms, and a left bundle branch block shape on an electrocardiogram could be responders to cardiac resynchronization therapy [2, 3]. As demonstrated in the PROSPECT study [4] and ECHO-CRT trial [5], echocardiography is unable to identify responders to this novel therapeutic strategy. Previous echocardiographic assessment of mechanical dyssynchrony was limited to regional LV wall information utilizing a tissue Doppler technique or M-mode calculation, although the heart is a three-dimensional moving muscle. Blood flow was also assessed using a pulse Doppler technique, which estimated the LV dysfunction using the time difference obtained from the blood stream at the LV and right ventricle inflow/outflow. Obviously, this was indirect information and did not critically reflect the whole LV wall motion. Therefore, the present author presumed that the accurate evaluation of LV dyssynchrony requires information for each wall of the heart during a consecutive cardiac cycle, particularly to determine the suitability of resynchronization therapy.

In the present study, it was hypothesized that the centroid of the LV reflects a cardiac wall motion because this technique requires the spatial coordinates of each endocardial position on the LV wall with time information during a cardiac cycle. Therefore, the locus of the centroid could include information on each regional area, such as the presence of interstitial/replacement fibrosis which limits LV contraction. This study investigated the role of the locus of the centroid in the assessment of abnormal LV wall motion as a novel approach differentiated from previous methods.

Methods

Study population

Continuous digital videos of 633 patients, which were obtained from the clinical echocardiography laboratory from September 2016 to August 2017, were utilized in this study. Cases of dilated cardiomyopathy (DCM) and old myocardial infarction (OMI) with aneurysm were evaluated. Cases of valvular heart disease, OMI without aneurysm, congenital structure cardiac disease, pulmonary hypertension, and those with images of poor quality were excluded from the study. The remaining videos that showed normal wall motion (NWM) of the LV were also used in this study as control.

The protocol of this retrospective study was approved by the SOYOKAZE CVD ethics committee (soyokaze-cvd, 2018-03). The purpose of this study was conveyed to the patients on the information

board and the website homepage of the clinic. An opt-out option was provided to patients who did not wish to participate in the study.

Two-dimensional tissue tracking system of the LV

Audio/video interleave files, obtained during one cardiac cycle using a trans-thoracic echocardiography equipped with a high-resolution sector probe (AVIUS; Hitachi Ltd., Tokyo, Japan), were evaluated. The two-dimensional speckle tracking algorithm (Hitachi Ltd.) is a pattern-matching method which forwards dozens of pixels into the region of interest (1 cm^2) through an off-line system using an application termed '%WT' programmed in e-Tool viewer (Hitachi Ltd.) [6, 7]. In this off-line system, approximately 50 points were automatically allocated on the manually traced line as the border of the endocardium. The coordinates of each point, which were followed frame by frame during one cardiac cycle, were saved as a comma-separated value file.

Locus of the centroid of the LV

The locus of the centroid of the LV was subsequently calculated through each frame image using an original application. The centroid of the three-dimensional LV was identified as the middle point between the centroid of the four-chamber image and that of the two-chamber image. The locus of the centroid of the three-dimensional LV was also shown on the same sheet.

Statistical analysis

The normally distributed continuous data are shown as mean values ± standard deviation. Non-normally distributed data are shown as medians with the first and third quartile values. Data with exponential distribution were logarithmically converted to obtain a normal distribution. Quantitative data were evaluated using one-way analysis of variance, with post-hoc analysis utilizing Tukey's method. Qualitative data were assessed through Fisher's exact test. Non-parametric data for each group were processed by Kruskal–Wallis analysis with a post-hoc method. A univariate linear regression analysis and a stepwise multiple linear regression analysis were applied to identify the independent predictors of the LVEF. A p-value < 0.05 denoted a statistically significant association in the final model.

All statistical analyses were performed with EZR (Saitama Medical Center, Jichi Medical University, Saitama, Japan), which is a graphical user interface for R (The R Foundation for Statistical Computing, Vienna, Austria). More precisely, it is a modified version of R commander designed to include additional statistical functions frequently used in biostatistics [8].

Results

A total of 260 patients were evaluated in this study. Patient background information is summarized in Table 1. The findings of physiological examination and a biomarker analysis for each group are summarized in Table 2.

Table 1
Background information of patients in each group

	DCM group	OMI group	NWM group	p-value
N	27	45	188	
Age, years (mean ± SD)	71 ± 11	72 ± 11	62 ± 16	7.24E-06
Sex, Female/Male, N	9/18	4/41	103/85	1.26E-08
Medication				
β-blocker	22 (81%)	33 (73%)	54 (29%)	1.03E-11
ACE-I/ARB	12 (44%)	21 (47%)	77 (41%)	0.835
Calcium-antagonist	9 (33%)	13 (29%)	66 (35%)	0.7704
Digitalis	2 (7%)	1 (2%)	0	0.0114
Diuretics	9 (33%)	20 (44%)	4 (2%)	1.03E-14
Anti-aldosterone	9 (33%)	12 (27%)	7 (6%)	5.21E-08
α-blocker	4 (15%)	4 (9%)	35 (17%)	0.3017
Nitrate	0	6 (13%)	3 (2%)	0.00349
Statin	17 (63%)	34 (76%)	89 (47%)	0.0016

ACE-I, angiotensin-converting enzyme inhibitor; ARB, angiotensin II receptor blocker; DCM, dilated cardiomyopathy; NWM, normal wall motion; OMI, old myocardial infarction; SD, standard deviation

Table 2
Physiological examination and biomarker data for each group

	DCM group	OMI group	NWM group	p-value
Echocardiography				
LVDd (mm)	57.7 ± 5.4	57.8 ± 8.7	48.1 ± 4.6	5.86E-27
LVDs (mm)	44.1 ± 6.0	43.7 ± 10.4	29.9 ± 5.0	6.12E-39
LVEDV (ml)	127.4 ± 40.1	137.5 ± 41.2	93.0 ± 28.0	8.49E-17
LVESV (ml)	73.1 ± 26.5	85.1 ± 34.7	36.0 ± 12.8	1.46E-40
LVEF (%)	43.5 ± 7.3	37.7 ± 11.3	61.3 ± 5.4	1.31E-61
Electrocardiography				
AF/NSR	7/20	3/42	1/187	1.12E-06
QRS width (ms)	106.2 ± 19.1	106.6 ± 21.2	94.9 ± 12.8	7.74E-07
Biomarker				
NT-proBNP (pg/ml)	1,712.7 ± 2,349.7	1,155.2 ± 1,147.6	121.2 ± 108.9	1.56E-19

Data are presented as the mean ± standard deviation.

AF, atrial fibrillation; DCM, dilated cardiomyopathy; LVDd, left ventricular diameter of the diastole; LVDs, left ventricular diameter of the systole; LVEDV, left ventricular end-diastolic volume; LVEF; left ventricular ejection fraction; LVESV; left ventricular end-systolic volume; NSR; normal sinus rhythm; NT-proBNP, N-terminal pro-brain natriuretic peptide; NWM, normal wall motion; OMI, old myocardial infarction

Representative images of the centroid of the LV in each group are demonstrated in Fig. 1. Firstly, the locus of the centroid that belonged to the NWM group had rapidly moved toward the anterior portion during the early systolic phase; thereafter, it shifted toward the apical direction. Subsequently, it returned to the original position through a diastolic relaxation phase and an atrial contraction stage; during this phase, the centroid moved in the counterclockwise direction on the same sheet frame by frame. Consequently, the locus of the centroid of the NWM group showed a horizontal inverted β shape. In the DCM group, the centroid of the three-dimensional LV showed a box-like shape and rotated clockwise; counterclockwise rotation was observed in the other groups. The locus image of the OMI group showed a crashed inverted β shape.

In the disease groups, the actual locus length of the centroid and the box volume were not significantly different among the groups (Figs. 2a, 2b). These were calculated from the x-, y-, z- transferred distance which the centroid of the three-dimensional LV had moved toward each direction during one cardiac cycle. However, when corrected by the LV end-systolic volume (LVESV), the length of the locus of the centroid of the DCM group (median value: 0.168 mm^{-2} [0.150–0.195 mm^{-2}]) and OMI group (mean value: 0.159 mm^{-2} [0.120–0.220 mm^{-2}]) was significantly shorter than that of the NWM group (median value: 0.379

mm^{-2} [0.305–0.493 mm^{-2}]; p = 7.85e-26) (Fig. 2c). The corrected box volume of the abnormal wall motion groups (median value, DCM group: 0.007 [0.004–0.010]; OMI group: 0.008 [0.004–0.006]) was also smaller than that calculated in the NWM group (median value: 0.011 [0.007–0.015]; p = 1.20e-8) when corrected by LVESV (Fig. 2d).

In the DCM group, the locus length of the centroid for the lateral and antero-posterior directions was longer than that of the NWM group (Figs. 3a, 3b); nevertheless, the length for the longitudinal direction was shorter than that of the NWM group (Fig. 3c). When these data were corrected by LVESV, the lengths were significantly reduced compared with those obtained from the NWM group (Figs. 3d, 3e). The corrected longitudinal length of the abnormal wall motion groups was markedly reduced compared with that of the NWM group (Fig. 3f).

The maximum acceleration of the LV centroid obtained for the DCM group (median value: 698 mm/s^2 [547–775 mm/s^2]) and OMI group (median value: 724 mm/s^2 [565–965 mm/s^2]) were reduced compared with that of the NWM group (median value: 878 mm/s^2 [713–1112 mm/s^2]; p = 7.49e-7) (Fig. 4a). On the other hand, the minimum acceleration of the LV centroid of the abnormal wall motion groups (median value, DCM group: −624 mm/s^2 [− 522−−776 mm/s^2]; OMI group: −589 mm/s^2 [− 507–804 mm/s^2]) was higher than that of the NWM group (median value: −826 mm/s^2 [− 668−−974 mm/s^2]; p = 4.12e-7) (Fig. 4b). When the acceleration values were corrected by LVESV, those of the abnormal wall motion groups were more markedly reduced compared with those of the NWM group (Figs. 4c, 4d).

In the univariate analysis, the transfer distance for the lateral direction, total distance of centroid movement during one cardiac cycle, maximum and minimum accelerations of the LV centroid, QRS duration, and value of the N-terminal pro-brain natriuretic peptide were associated with LVEF (Table 3). However, when the data concerning the distance, volume, velocity and acceleration of the centroid were corrected by LVESV, all data included in Table 3 were related to LVEF. The QRS duration, total distance of centroid movement, maximum velocity, and mean acceleration of the LV centroid were excluded from the multivariate analysis because these data were considered variance inflation factors. Finally, a multiple linear regression analysis with stepwise methods revealed that the N-terminal pro-brain natriuretic peptide and an antero-posterior shift of the LV centroid were strong predictors of the LVEF (multiple R^2: 0.6882; adjusted R^2: 0.6818; $p \leq 2.2e\text{-}16$) (Table 4).

Table 3
Univariate analysis for the prediction of LVEF

Factor	β	95% CI		SE	t-value	p-value
		Lower	Upper			
Log(Transfer distance for the lateral direction of the centroid)	−16.75786	−26.6021	−6.913633	4.999098	−3.352177	9.22E − 04
Log(Transfer distance for the A-P direction of the centroid)	−3.143287	−14.84097	8.5544	5.94032	−0.5291443	5.97E − 01
Log(Transfer distance for the longitudinal direction of the centroid)	11.56642	−0.7904423	23.92329	6.275064	1.843236	6.64E − 02
Distance of centroid movement during one cardiac cycle	0.5832442	0.008625036	1.157863	0.2918031	1.998759	4.67E − 02
Log(Total moving box volume of the centroid)	−3.279045	−8.629779	2.071689	2.71721	−1.206769	2.29E − 01
Mean velocity of the centroid during one cardiac cycle	0.4976478	−0.02678432	1.02208	0.2663172	1.868628	6.28E − 02
Maximum velocity of the centroid during one cardiac cycle	0.1186465	−0.02698795	0.2642809	0.07395609	1.604283	1.10E − 01
Log(Minimum velocity of the centroid during one cardiac cycle)	−3.740764	−9.106621	1.625092	2.7248896	−1.372813	1.71E − 01

A-P, antero-posterior; CI, confidence interval; LCG, locus of the center of gravity; Log; logarithmic; LVEF, left ventricular ejection fraction; LVESV, left ventricular end-systolic volume; NT-proBNP, N-terminal pro-brain natriuretic peptide; SD, standard error

Factor	β	95% CI		SE	t-value	p-value
		Lower	Upper			
Log(Mean acceleration of the centroid during one cardiac cycle)	4.566414	−1.274704	10.40753	2.966237	1.539464	1.25E − 01
Log(Maximum acceleration of the centroid during one cardiac cycle)	20.29745	10.74705	29.84785	4.849887	4.185139	3.91E − 05
Log(Minimum acceleration of the centroid during one cardiac cycle)	−21.99373	−31.09265	−12.8948	4.620616	−4.7599121	3.23E − 06
Log(QRS duration)	−52.34276	−73.98228	−30.70323	10.98898	−4.763202	3.18E − 06
Log(NT-proBNP)	−11.59067	−13.67674	−9.504603	1.059187	−10.94299	4.99E − 23
Corrected by LVESV						
Log(Transfer distance for the lateral direction of the centroid/LVESV)	36.96853	31.87738	42.05969	2.585389	14.29902	1.50E − 34
Log(Transfer distance for the A-P direction of the centroid/LVESV)	36.40963	32.22252	40.59674	2.126299	17.12347	2.00E − 44
Transfer distance for the longitudinal direction of the centroid /LVESV	470.58136	411.81713	529.34559	29.841655	15.76928	1.09E − 39
Distance of centroid movement during one cardiac cycle/LVESV	56.67316	50.37252	62.97379	3.19959	17.71263	1.76E − 46

A-P, antero-posterior; CI, confidence interval; LCG, locus of the center of gravity; Log; logarithmic; LVEF, left ventricular ejection fraction; LVESV, left ventricular end-systolic volume; NT-proBNP, N-terminal pro-brain natriuretic peptide; SD, standard error

Factor	β	95% CI		SE	t-value	p-value
		Lower	Upper			
Log(Total moving box volume of the centroid /LVESV)	20.89161	16.75028	25.03295	2.103054	9.933941	6.68E − 20
Log(Mean velocity of the centroid during one cardiac cycle/LVESV)	40.0867	36.38057	43.79283	1.882046	21.29953	8.86E − 59
Log(Maximum velocity of the centroid during one cardiac cycle/LVESV)	38.39226	34.70603	42.07848	1.8719381	20.50936	4.14E − 56
Log(Minimum velocity of the centroid during one cardiac cycle /LVESV)	15.65795	11.8638	19.4521	1.926744	8.126638	1.85E − 14
Log(Mean acceleration of the centroid during one cardiac cycle /LVESV)	18.75454	15.38623	22.12284	1.710494	10.9644	3.25E − 23

A-P, antero-posterior; CI, confidence interval; LCG, locus of the center of gravity; Log; logarithmic; LVEF, left ventricular ejection fraction; LVESV, left ventricular end-systolic volume; NT-proBNP, N-terminal pro-brain natriuretic peptide; SD, standard error

Factor	β	95% CI		SE	t-value	p-value
		Lower	Upper			
Log(Maximum acceleration of the centroid during one cardiac cycle /LVESV)	30.88431	27.51855	34.25007	1.709201	18.069445	1.01E − 47
Log(Minimum acceleration of the centroid during one cardiac cycle /LVESV)	−30.3035	−33.56723	−27.03978	1.657384	−18.283931	1.82E − 48

A-P, antero-posterior; CI, confidence interval; LCG, locus of the center of gravity; Log; logarithmic; LVEF, left ventricular ejection fraction; LVESV, left ventricular end-systolic volume; NT-proBNP, N-terminal pro-brain natriuretic peptide; SD, standard error

Table 4
Stepwise multiple linear regression analysis for the prediction of the LVEF

Factor	β	95% CI		SE	t-value	p-value
		Lower	Upper			
Intercept	109.73	87.16	132.29	11.45	9.58	1.20E − 18
Log(NT.proBNP)	−5.68	−7.46	−3.89	0.91	−6.26	1.80E − 09
Log(Transfer distance for the A-P direction of the centroid /LVESV)	23.32	15.76	30.87	3.84	6.08	4.70E − 09
Log(Transfer distance for the lateral direction of the centroid /LVESV)	13.14	7.28	23.08	4.01	3.78	1.90E − 04
Log(Total moving box volume of the centroid /LVESV)	−10.70	−16.07	−5.33	2.73	−3.93	1.10E − 04

A-P, antero-posterior, CI, confidence interval; Log, logarithmic; LVEF; left ventricular ejection fraction, LVESV; left ventricular end-systolic volume, NT-proBNP; N-terminal pro-brain natriuretic peptide, SE, standard error

Discussion

The present study demonstrated that the LV centroid of the NWM group had moved like a mirror image of a β shape in a counterclockwise direction. In case of abnormal wall motion (e.g., dyssynchrony associated with DCM or LV aneurysm caused by an OMI), the corrected distance for any direction of the locus of the centroid by LVESV was significantly reduced compared with that noted for the NWM group, especially in

the longitudinal direction. The LV centroid had to shift toward the anterior direction in an early phase of LV contraction to increase the LVEF.

In patients with an extended LV chamber, the length which the LV centroid had moved during one cardiac cycle was limited to the enlarged cavity. This is because the cardiac muscle is confined in the cardiac sac, which is constructed by a tight fibrous membrane. To obtain sufficient stroke volume from the LV cavity, the LV centroid had to shift to the frontal position into the LV during the early contraction phase. This is because the blood stream had to be directed toward a LV outflow rather than a LV inflow positioned in a mitral ring. After moving toward the apical direction, it returned to the original position with two loose loops, which might have been caused by the cardiac translation of a diastolic phase and an atrial kick. Furthermore, the box volume calculated from the locus of the LV centroid to the LVESV was reversely correlated with the LVEF. This indicated that the floating motion of the LV centroid had not contributed to an increase in the LVEF.

The evaluation of LV wall motion (e.g., asynergy or dyssynchrony) using echocardiography is often subjective and depends on the experience of the physicians and expert technicians. It has been reported that strain is a good evaluator of the regional asynergy of ischemic heart disease [9, 10, 11]. In contrast, there are no standard markers available for the evaluation of mechanical dyssynchrony. Several studies assessed mechanical dyssynchrony using a tissue Doppler method [12, 13, 14], the time difference between the opposite sites using a M-mode technique [15], and the time discrepancy between the pre-ejection time of both ventricles or the LV filling time for a R-R interval [16]. However, the PROSPECT trial demonstrated that the aforementioned echocardiographic parameters failed to identify the responders to cardiac re-synchronization therapy [4] because those evaluations were restricted to local or indirect information of the LV wall. The results of this study proposed the LV centroid as a novel approach, which requires information on each point of the LV endocardium and each time point during a cardiac cycle. This method depends on the spatial and temporal information of the whole LV endocardium of the moving heart rather than selected information from a part of the LV and a limited time. Based on these reasons, this novel approach may contribute to the selection of patients with mechanical dyssynchrony who could respond to cardiac resynchronization therapy.

In conclusion, the locus of the centroid of the LV associated with abnormal contraction of the heart did not resemble the mirror image of a β shape. Furthermore, the corrected antero-posterior shift of the LV centroid by LVESV was a strong predictor of the LVEF. The present evidence demonstrated that these are important factors for maintaining sufficient systolic volume.

Limitations

In this study, the LV centroid calculated from two orthogonal views using a two-dimensional tracking method was utilized as a three-dimensional LV gravity. If a real-time three-dimensional speckle tracking system was available, the association with the LV centroid could have been examined in more detail.

Abbreviations

DCM, dilated cardiomyopathy

EchoCRT, echocardiography guided cardiac resynchronization therapy

LV, left ventricle

LVEF, left ventricular ejection fraction

LVESV, left ventricular end-systolic volume

NWM, normal wall motion

OMI, old myocardial infarction

PROSPECT, predictors of response to cardiac resynchronization therapy

Declarations

Ethics approval and consent to participate: The protocol of this retrospective study was approved by the SOYOKAZE CVD ethics committee (soyokaze-cvd, 2018-03). The purpose of this study was conveyed to the patients on the information board and the website homepage of the clinic. An opt-out option was provided to patients who did not wish to participate in the study.

Consent for publication: Not applicable.

Availability of data and materials: The datasets used and/or analyzed during the current study are available from the corresponding author on reasonable request.

Competing interests: Not applicable.

Funding: Not applicable.

Authors' contributions: This paper was prepared by a single author.

Acknowledgements: The author especially thanks Mr. H. Hayashi for programing this original application.

References

1. Mitchell C, Rahko PS, Blauwet LA, Canaday B, Finstuen JA, Foster MC, et. al. Guidelines for Performing a Comprehensive Transthoracic Echocardiographic Examination in Adults: Recommendations from the American Society of Echocardiography. J Am Soc Echocardiogr. 2019; 32:1–64. doi: 10.1016/j.echo.2018.06.004.
2. Ponikowski P, Voors AA, Anker SD, Bueno H, Cleland JGF, Andrew J. S, *et al*, 2016 ESC Guidelines for the diagnosis and treatment of acute and chronic heart failure. Eur H J 2016;37:2129–2200.

3. Seferovic PM, Ponikowski P, Anker SD, Bauersachs J, Chioncel O, Cleland JGF, *et al*, Clinical practice update on heart failure 2019: pharmacotherapy, procedures, devices and patient management. An expert consensus meeting report of the Heart Failure Association of the European Society of Cardiology. Eur H Fail 2019. doi:10.1002/ejhf.1531
4. Chung ES, Leon AR, Tavazzi L, Sun JP, Nihoyannopoulos P, Merlino J, *et al*, Results of the predictors of response to CRT (PROSPECT) trial. Circulation. 2008; 20:117:2608-16. doi: 10.1161/CIRCULATIONAHA.107.743120.
5. Ruschitzka F, Abraham WT, Singh JP, Bax JJ, Borer JS, Brugada J, *et al*, EchoCRT Study Group, Cardiac-resynchronization therapy in heart failure with a narrow QRS complex. N Engl J Med. 2013;369:1395-405. doi: 10.1056/NEJMoa1306687.
6. Baba H, Mori O, Miyaoka T, Development of 2D tissue trecking. MEDIX 2005; 43:19-22.
7. Miyoshi A, Nakamura Y, Kazatani Y, Ito H. The feasibility of substituting left atrial wall strain for flow velocity of left atrial appendage. Acta Cardiol 2018; 73:125-130. doi: 10.1080/00015385.2017.1351242
8. Kanda Y. Investigation of the freely available easy-to-use software 'EZR' medical statistics. Bone Marrow Transplant. 2013; 48:452-8.
9. Kusunose K, Yamada H, Nishio S, Mizuguchi Y, Choraku M, Maeda Y, *et. al*., Validation of longitudinal peak systolic strain by speckle tracking echocardiography with visual assessment and myocardial perfusion SPECT in patients with regional asynergy. *Circ J* 2011; 75:141-147. DOI; https://doi.org/10.1253/circj.CJ-10-0551.
10. Anwar A, Nosir Y, Alasnag M, Llemit MA, Elhagoly AA, Chamsi-Pasha H, Quantification of left ventricular longitudinal strain by two-dimensional speckle tracking: A comparison between expert and non-expert readers. Int J Cardiovasc Imaging 2013; 29:1451-8. doi: 10.1007/s10554-013-0247-1.
11. Stankovic I, Putnikovic B, Cvjetan R, Milicevic P, Panic M, Kalezic-Radmili T, *et al*, Visual assessment vs. strain imaging for the detection of critical stenosis of the left anterior descending coronary artery in patients without a history of myocardial infarction. Eur Heart J Cardiovasc Imaging 2015; 16:402-9. doi: 10.1093/ehjci/jeu206.
12. Yu CM, Fung WH, Lin H, Zhang Q, Sanderson JE, Lau CP, Predictors of left ventricular reverse remodeling after cardiac resynchronization therapy for heart failure secondary to idiopathic dilated or ischemic cardiomyopathy. Am J Cardiol. 2003; 91:684-8. doi: 10.1016/s0002-9149(02)03404-5.
13. Bax JJ, Bleeker GB, Marwick TH, Molhoek SG, Boersma E, Steendijk P, *et al*, Left ventricular dyssynchrony predicts response and prognosis after cardiac resynchronization therapy. J Am Coll Cardiol. 2004; 44:1834-40.doi: 10.1016/j.jacc.2004.08.016.
14. Yu CM, Chan YS, Zhang Q, Yip GWK, Chan CK, Kum LCC, *et al*, Benefits of cardiac resynchronization therapy for heart failure patients with narrow QRS complexes and coexisting systolic asynchrony by echocardiography**.** J Am Coll Cardiol. 2006; 48:2251-7. doi: 10.1016/j.jacc.2006.07.054.
15. Pitzalis MV, Iacoviello M, Romito R, Massari F, Rizzon B, Luzzi G, *et al*, Cardiac resynchronization therapy tailored by echocardiographic evaluation of ventricular asynchrony. J Am Coll Cardiol. 2002;

40:1615-22. doi: 10.1016/s0735-1097(02)02337-9.

16. S Cazeau, P Bordachar, G Jauvert, A Lazarus, C Alonso, M C Vandrell, *et al*, Echocardiographic modeling of cardiac dyssynchrony before and during multisite stimulation: a prospective study. Pacing Clin Electrophysiol. 2003:137-43. doi: 10.1046/j.1460-9592.2003.00003.x.

Figures

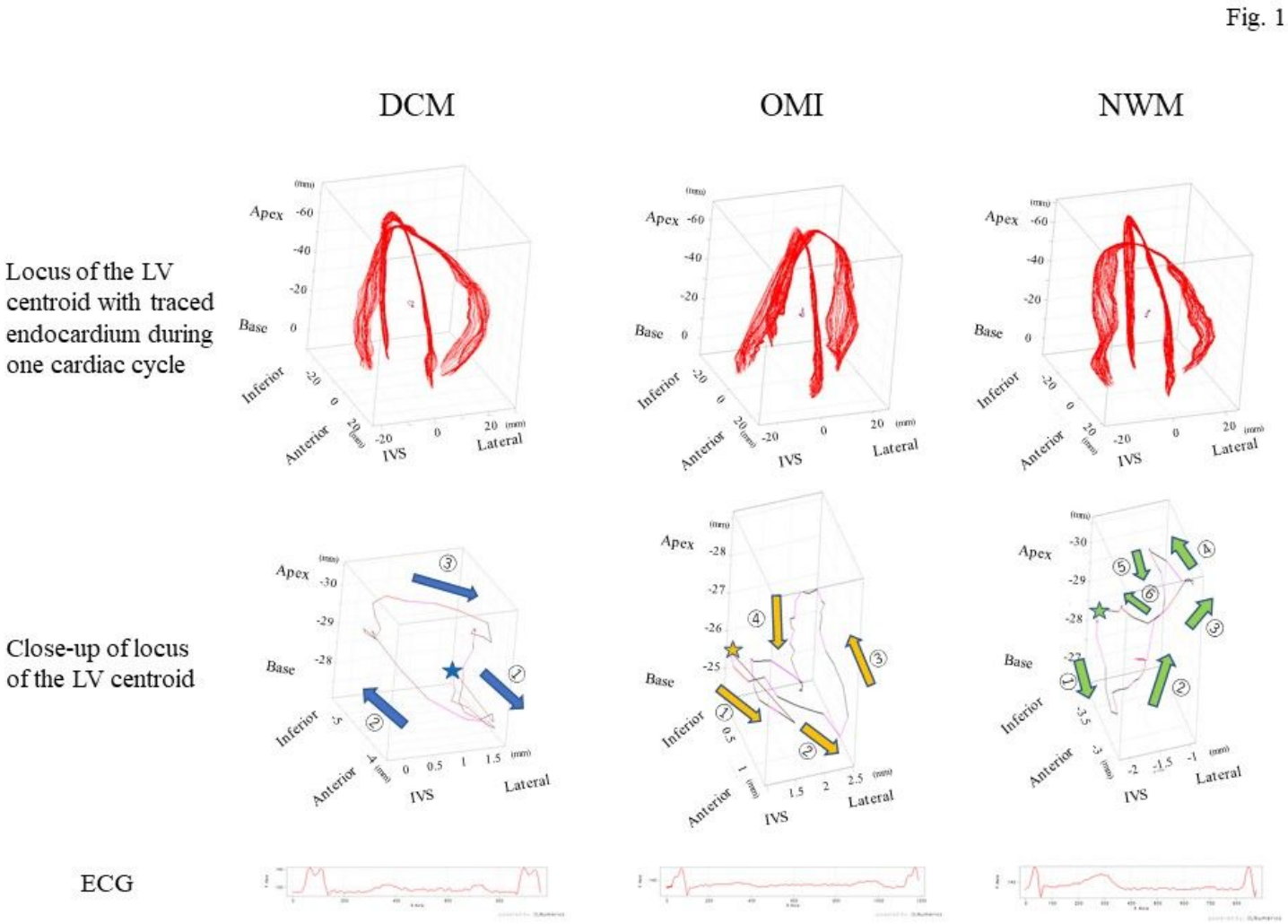

Figure 1

Representative images of the locus of the centroid of the left ventricle for each group. The top panels show the outline of the endocardium (red lines) obtained from an apical four-chamber view (x-axis) with a two-chamber view (y-axis) of the left ventricle drawn in the same cubic together with all frames of the endocardium lines accompanied by the locus of the centroid of the left ventricle. The middle panels indicate the close-up of the locus of the centroid of the left ventricle. The stars in each illustration indicate a starting point on a systolic period, which revealed the starting point of the QRS spike on the electrocardiogram. Normal left ventricular wall motion showed that the centroid of the left ventricle shifted

to the frontal portion during an early systolic phase (green arrow 1, thereafter that point rapidly moved toward the apical site (green arrows 2 and 3). Subsequently, it returned to the starting point with two loose loops during a diastolic phase and an atrial contraction (green arrows 4–6), resembling a mirror image of a β shape. The DCM group showed movement in a swinging motion on the box like a load with clockwise rotation (blue arrows). The OMI group showed that the locus formed a crashed inverted β shape with counterclockwise rotation (brown arrows). The bottom panels show the electrocardiogram of each group. DCM, dilated cardiomyopathy; ECG, electrocardiogram; IVS, interventricular septum; LV, left ventricle; NWM, normal wall motion; OMI, old myocardial infarction.

Fig. 2

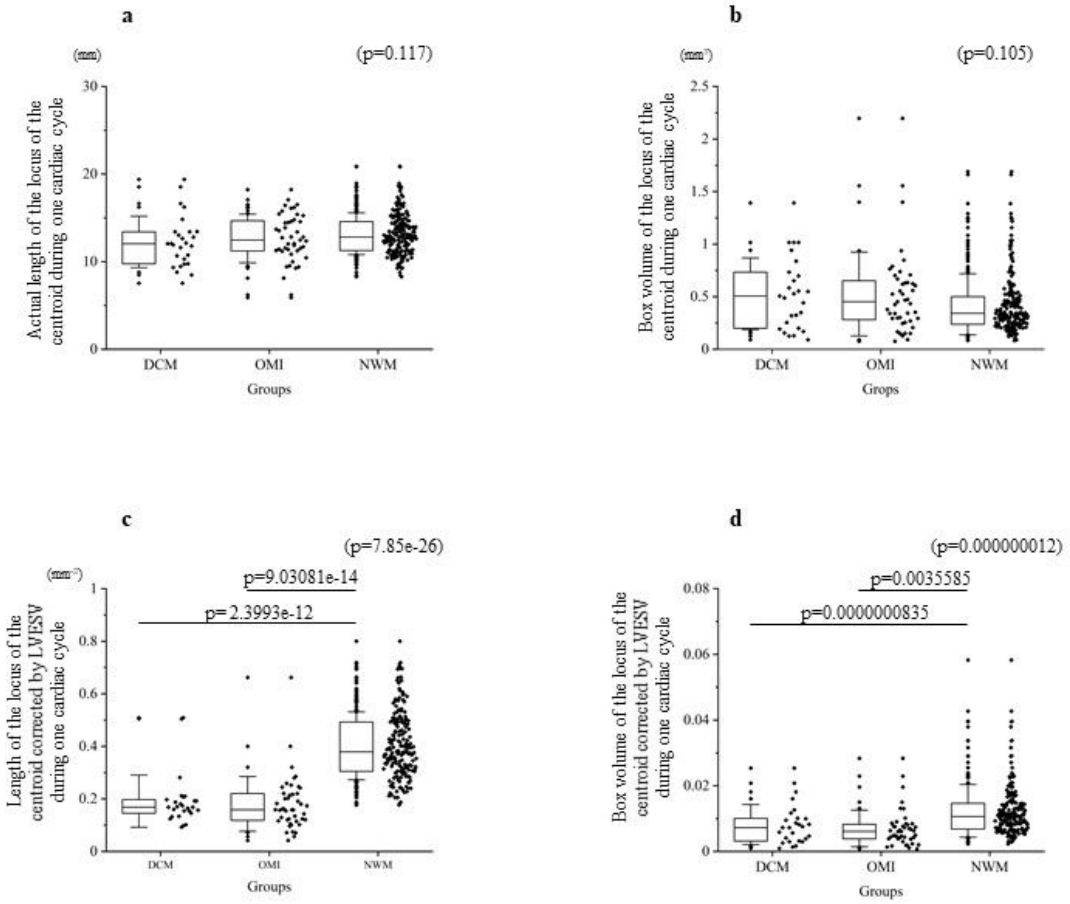

Figure 2

The length and moving space of the locus of the centroid of the left ventricle for each group. The top panels show the actual length (a) and calculated box volume from the x-, y-, z-moving length (b). There was no significant difference among the groups. The bottom panels show the corrected data by LVESV. The corrected length of the locus of the centroid of the left ventricle (c) and the corrected volume (d) were significantly reduced in the DCM and OMI groups. DCM, dilated cardiomyopathy; LVESV, left ventricular end-systolic volume; NWM, normal wall motion; OMI, old myocardial infarction.

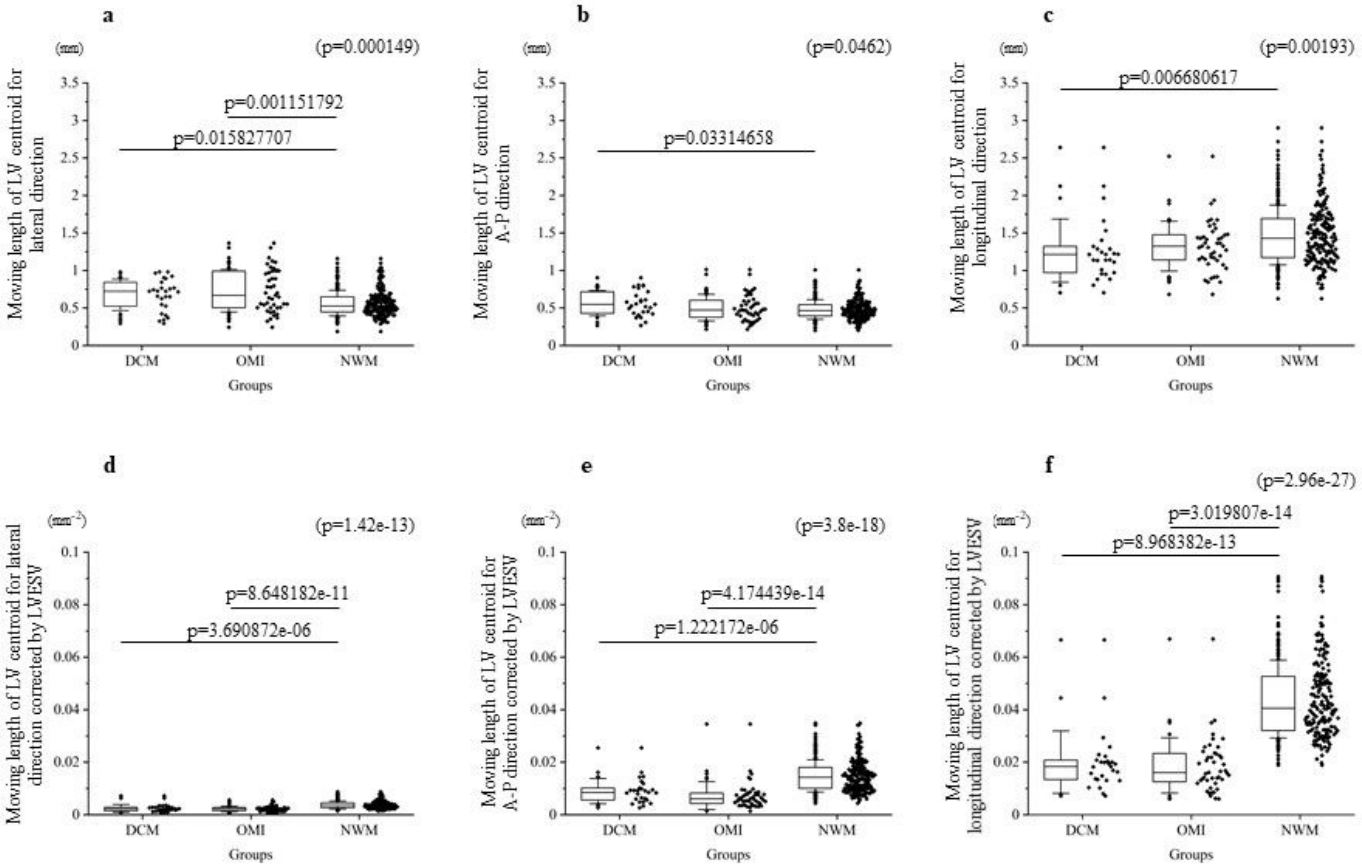

Figure 3

Comparison of the moving length of the locus of the centroid toward each direction. The top panels indicate the actual length for each direction: (a) lateral direction; (b) A-P direction; and (c) longitudinal direction. The bottom panels show the corrected length by LVESV. (d) shows the corrected length for the lateral direction by LVESV. (e) shows the corrected length for the antero-posterior direction by LVESV. (f) indicates the corrected length for the longitudinal direction by LVESV. The corrected lengths of the locus of the centroid of the left ventricle by LVESV for each direction were clearly suppressed compared with those recorded in the NWM group. A-P, antero-posterior; DCM, dilated cardiomyopathy; LV, left ventricle; LVESV, left ventricular end-systolic volume; NWM, normal wall motion; OMI, old myocardial infarction.

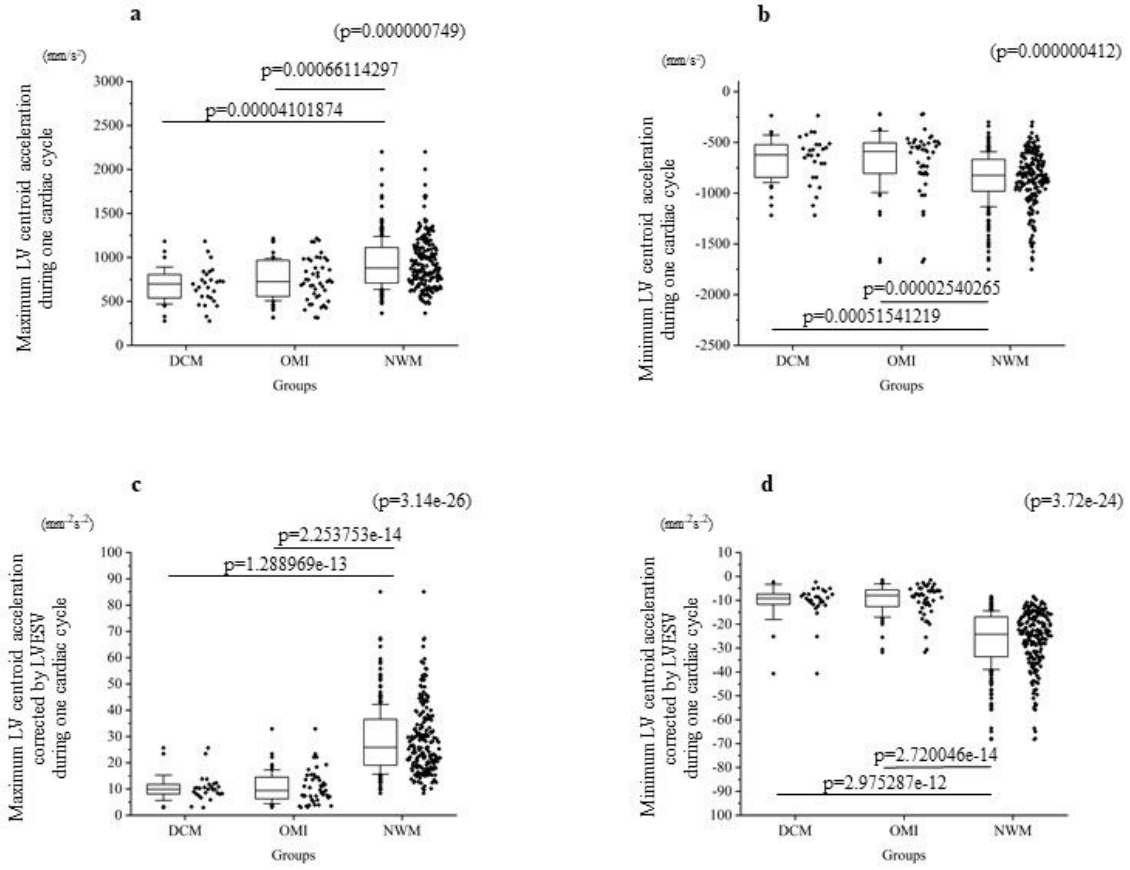

Figure 4

Comparison of the maximal and minimum accelerations of the locus of the centroid of the left ventricle among the groups. The top panels indicate the real data ([a] for maximum acceleration, [b] for minimum acceleration), while the bottom panels show the corrected data by LVESV ([c] for the corrected maximal acceleration, [d] for the corrected minimum acceleration). When corrected by LVESV, the maximum and minimum accelerations in the abnormal wall motion groups were clearly reduced compared with those measured in the NWM group. DCM, dilated cardiomyopathy; LV, left ventricle; LVESV, left ventricular end-systolic volume; NWM, normal wall motion; OMI, old myocardial infarction.